

SKI Report 2004:05
SSI Report 2004:01

Research

Further AMBER and Ecolego Intercomparisons

Philip Maul
Peter Robinson
Robert Broed
Rodolfo Avila

January 2004



Statens strålskyddsinstitut
Swedish Radiation Protection Authority

ISSN 1104-1374
ISSN 0282-4434
ISRN SKI-R-04/05-SE

SKi

SKI/SSI perspective

Background

As part of preparations for review of future license applications, the Swedish Nuclear Power Inspectorate (SKI) and Swedish Radiation Protection Authority (SSI) are developing their capabilities of doing radionuclide transport calculations. For this purpose SKI and SSI have developed the software program AMBER and Ecolego respectively.

The AMBER compartmental modelling software has been used by Quintessa in undertaking Performance Assessment (PA) calculations for SKI for the last four years. In particular, it was used in helping to identify key issues in the safety case for SFR 1. SSI and the Norwegian Radiation Protection Authority (NRPA) are supporting the development of Ecolego which is based on the Matlab/Simulink general purpose modelling software and provides a user-friendly Graphical User Interface (GUI) which is particularly suitable for undertaking PA calculations.

Purpose of the project

Based on calculation cases considered in SKB's SR 97, intercomparison calculations using AMBER and Ecolego was done in a previous project (SKI, SSI, 2003). The reasons for undertaking such intercomparisons were to give confidence in the use of AMBER and Ecolego for whole system PA calculations for a deep repository. And to provide SKI and SSI with an understanding of some of the technical issues raised by seeking to repeat the SR 97 calculations with different models and software.

In order to gain more information on the comparisons between the two codes, additional intercomparisons have been undertaken using input data from the Vault Safety Case originally undertaken as part of an IAEA research project (ISAM).

Results

The comparisons between the AMBER and Ecolego calculations for the ISAM vault safety case have shown excellent agreement. Calculations at specified times generally agree to around three significant figures, and calculations of peak radionuclide fluxes and concentrations agree to two significant figures. This agreement is particularly good given the large number of model compartments and the inclusion of decay changes of up to six members.

Project information

SKI project manager: Benny Sundström.

SKI project identification number: 14.9-030741/03138

SSI project manager: Shulan Xu.

Relevant reports:

Radionuclide Transport Modelling: Current Status and Future Needs - Seminar Johannesburg, Sweden, 6-8 November 2001 Synthesis, Work Group Reports and Extended Abstracts, Swedish Nuclear Power Inspectorate, Stockholm, Sweden, 2002.

SKI, SSI, AMBER and Ecolego Intercomparisons using Calculations from SR97, SKI Report 2003:28, SSI report 2003:11, Statens kärnkraftinspektion, Statens strålskydds-institut, Stockholm, 2003.

Research

Further AMBER and Ecolego Intercomparisons

Philip Maul¹
Peter Robinson¹
Robert Broed²
Rodolfo Avila³

¹Quintessa Limited
Dalton House
Newtown Road
Henley-on-Thames
Oxfordshire RG9 1HG
United Kingdom

²Department of Physics
Center of Physics, Astronomy and Biotechnology
AlbaNova University Center
Stockholm University
SE-106 91 Stockholm
Sweden

³Facilia AB
Valsgärdevägen 12
SE-168 53 Bromma, Stockholm
Sweden

January 2004

This report concerns a study which has been conducted for the Swedish Nuclear Power Inspectorate (SKI) and the Swedish Radiation Protection Authority (SSI). The conclusions and viewpoints presented in the report are those of the author/authors and do not necessarily coincide with those of the SKI and the SSI.

Contents

SUMMARY	1
SAMMANFATTNING	3
1 INTRODUCTION	5
2 THE ISAM VAULT SAFETY CASE	7
2.1 SYSTEM DESCRIPTION	7
2.2 THE REPOSITORY SUB-MODEL	10
2.3 THE UNSATURATED GEOSPHERE SUB-MODEL	13
2.4 THE SATURATED GEOSPHERE SUB-MODEL	15
3 AMBER AND ECOLEGO CALCULATIONS	19
3.1 RADIONUCLIDE FLUXES FROM THE REPOSITORY	19
3.2 RADIONUCLIDE FLUXES FROM THE UNSATURATED ZONE	24
3.3 WELL WATER CONCENTRATIONS.....	28
4 CONCLUSIONS	33
REFERENCES	35

Summary

The AMBER compartmental modelling software is used by Quintessa in undertaking Performance Assessment (PA) calculations for SKI. SSI and NRPA are supporting the development of Ecolego which is based on the Matlab/Simulink general purpose modelling software for undertaking PA calculations.

Intercomparison calculations using AMBER and Ecolego have been undertaken based on calculation cases considered in SKB's SR97 assessment. The reasons for undertaking such intercomparisons included:

1. to give confidence in the use of AMBER and Ecolego for whole system PA calculations for a deep repository; and
2. to provide SKI and SSI with an understanding of some of the technical issues raised by seeking to repeat the SR97 calculations with different models and software.

Conclusions drawn from these intercomparisons included:

1. Both modelling packages successfully reproduced SKB's SR97 calculations for the near field, geosphere and biosphere.
2. AMBER and Ecolego calculations were typically in agreement to within one significant figure, but in several instances the SR97 documentation was not sufficiently clear to enable the implementation of the models in AMBER and Ecolego to be unambiguous.

In order to gain more information on the comparisons between the two codes, additional intercomparisons have been undertaken using input data from the Vault Safety Case originally undertaken as part of an IAEA research project (ISAM).

The comparisons between the AMBER and Ecolego calculations for the ISAM vault safety case have shown excellent agreement. Calculations at specified times generally agree to around three significant figures, and calculations of peak radionuclide fluxes and concentrations agree to two significant figures. This agreement is particularly good given the large number of model compartments and the inclusion of decay changes of up to six members.

The most important situation where agreement may not be as good as that generally found is where radionuclides have been subject to substantial losses due to radioactive decay; at times after the production of the radionuclide that are very much greater than the radionuclide half-life.

Sammanfattning

Modelleringsverktyget AMBER används av Quintessa i säkerhetsanalysberäkningar för SKI, SSI och statens strålevern i Norge (NRPA) stöder utvecklingen av Ecolego vilken är baserad på den kommersiella programvaran Matlab/Simulink och används för säkerhetsanalysberäkningar.

Jämförande beräkningar mellan AMBER och Ecolego har utförts baserat på beräkningsfall gjorda i SKB:s SR 97. Anledningen till att göra sådana jämförelser var:

1. att ge tillit i användandet av AMBER:s och Ecolego:s hela system för säkerhetsanalysberäkningar för ett djupförvar; och
2. att ge SKI och SSI kunskap om några av de tekniska frågeställningar som kan uppkomma när man försöker att upprepa SR 97 beräkningarna med olika modeller och programvaror.

De slutsatser som kunde dras från dessa jämförelser var:

1. Båda modellpaketen kunde framgångsrikt reproducera SKB:s SR 97 beräkningar för närområdet, geosfären och biosfären.
2. Beräkningsresultaten från AMBER och Ecolego överensstämde inom en siffrans noggrannhet, men i flera fall var dokumentationen i SR 97 inte tillräckligt tydlig för att entydigt kunna utnyttja modellerna i AMBER och Ecolego.

För att få ytterligare information angående jämförelser mellan de två koderna, har ytterligare jämförande beräkningar gjorts med ingångsdata tagna från säkerhetsredovisningen av förvar i bergrum ingående som en del av IAEA:s forskningsprogram (ISAM).

Jämförelserna av beräkningar utförda med AMBER och Ecolego för ISAMS:s säkerhetsredovisning av förvar i bergrum har visat utmärkta överensstämmelser. Beräkningarna vid angivna tidpunkter stämmer i allmänhet överens inom tre siffrors noggrannhet, och beräkningar av maximala flödet och koncentrationer av radionuklider stämmer överens med två siffrors noggrannhet. Denna överensstämmelse är särskilt god med tanke på de stora antalet modelleringsdelar och medtagna sönderfallskedjor med upp till sex nuklidmedlemmar.

Den mest betydelsefulla situationen där överensstämmelsen inte är lika bra som övriga fall är då radionuklider har haft möjligheten att sönderfalla; det vid tider som är mycket längre än radionuklidens halveringstid från det att den bildats.

1 Introduction

The AMBER compartmental modelling software (Enviros and Quintessa, 2003) is used by Quintessa in undertaking Performance Assessment (PA) calculations for SKI. SSI and NRPA are supporting the development of Ecolego (Avila et al. 2003) which is based on the Matlab/Simulink general purpose modelling software for undertaking PA calculations.

Intercomparison calculations using AMBER and Ecolego have been undertaken (SKI and SSI, 2003) based on calculation cases considered in SKB's SR97 assessment (SKB, 1999). The reasons for undertaking such intercomparisons included:

1. to give confidence in the use of AMBER and Ecolego for whole system PA calculations for a deep repository; and
2. to provide SKI and SSI with an understanding of some of the technical issues raised by seeking to repeat the SR97 calculations with different models and software.

Conclusions drawn from these intercomparisons included:

1. Both modelling packages successfully reproduced SKB's SR97 calculations for the near field, geosphere and biosphere.
2. AMBER and Ecolego calculations were typically in agreement to within one significant figure, but in several instances the SR97 documentation was not sufficiently clear to enable the implementation of the models in AMBER and Ecolego to be unambiguous.

Additional intercomparisons have now been undertaken using input data from the Vault Safety Case originally undertaken as part of an IAEA research project, ISAM (IAEA, 2001). A particular aim of this set of intercomparisons was to include calculations for decay chains; the SKB SR97 calculations only considered individual radionuclides.

This report is structured as follows:

In Section 2 the Vault Safety Case analysis is described, and its basis as a test case for AMBER-Ecolego intercomparisons defined.

In Section 3 details of the AMBER and Ecolego calculations are presented.

Finally, Section 4 summarises the main conclusions that can be drawn.

2 The ISAM Vault Safety Case

In this section details of those parts of the ISAM Vault Safety Case assessment relevant to the AMBER/Ecolego intercomparisons are given. Consideration is restricted to the leachate (liquid) transport pathway and to the compartmental modelling approach implemented in AMBER for the Vault Safety Case. No discussion is given on justifications for the model structures and parameter values; these can be found in IAEA (2001).

2.1 System Description

The conceptual model for leachate release in the ISAM Vault Safety Case consists of four parts, as shown in Figure 2.1.1.

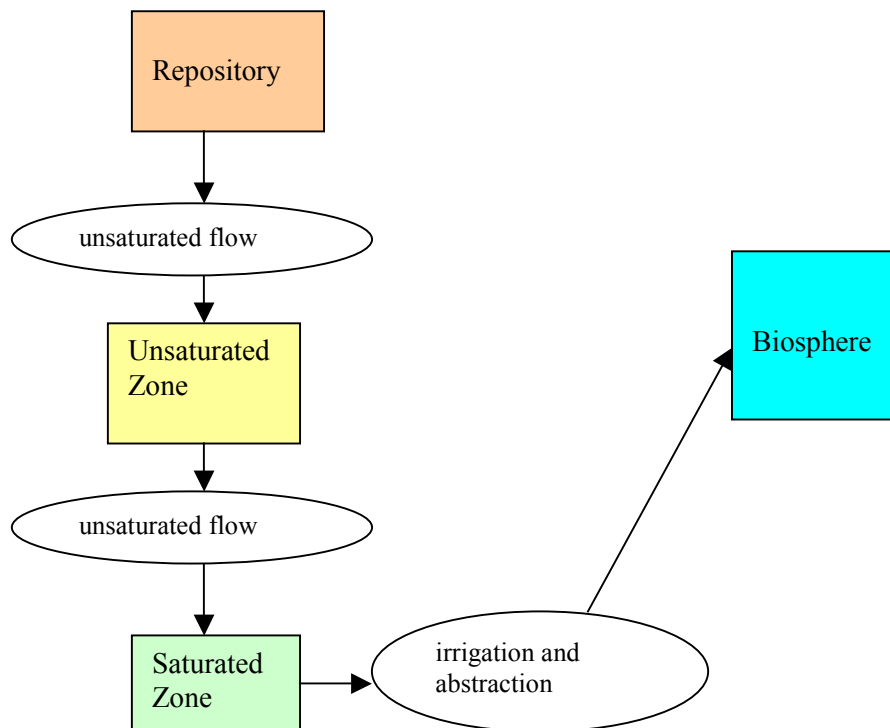


Figure 2.1.1 Sub-Models in the Vault Safety Case Assessment for Leachate Release.

Radionuclides are transported in unsaturated groundwater flow from the repository to the unsaturated zone and then to the saturated zone. The saturated zone includes a well from which water is abstracted and used for irrigation; this is the route for radionuclide transport to the biosphere sub-system. In the AMBER/Ecolego test calculations radionuclide transport in the Biosphere sub-model was not considered.

Table 2.1.1 gives details of the initial inventory in the waste, Table 2.1.2 shows the simplified radionuclide decay chains used in the calculations, and Table 2.1.3 gives the radionuclide decay constants that were used.

Table 2.1.1 Initial Inventory in the Waste.

Radionuclide	Inventory disposed (Bq)	Radionuclide	Inventory disposed (Bq)
H-3	1E+15	Cs-137	8E+15
C-14	1E+13	U-234	5E+10
Ni-59	2E+10	U-238	5E+10
Ni-63	1E+15	Pu-238	2E+10
Sr-90	1E+14	Pu-239	3E+10
Tc-99	3E+10	Pu-241	6E+11
I-129	6E+9	Am-241	2E+10

Table 2.1.2 Radionuclide Decay Chains.

Head of chain	Daughters
U-238	U-234 → Th-230 → Ra-226 → Pb-210 → Po-210
Pu-238	U-234 → Th-230 → Ra-226 → Pb-210 → Po-210
Pu-239	U-235 → Pa-231 → Ac-227
Pu-241	Am-241 → Np-237 → Pa-233 → U-233 → Th-229

Table 2.1.3 Radionuclide Decay Constants.

Radionuclide	Decay Constant (y ⁻¹)	Radionuclide	Decay Constant (y ⁻¹)
H-3	5.59E-02	Th-230	9.00E-06
C-14	1.21E-04	Pa-230	2.11E-05
Ni-59	9.19E-06	Pa-233	9.38E+00
Ni-63	7.22E-03	U-233	4.36E-06
Sr-90	2.38E-02	U-234	2.83E-06
Tc-99	3.25E-06	U-235	9.85E-10
I-129	4.41E-08	U-238	1.55E-10
Cs-137	2.31E-02	Np-237	3.24E-07
Pb-210	3.11E-02	Pu-238	7.90E-03
Po-210	1.83E+00	Pu-239	2.88E-05
Ra-226	4.33E-04	Pu-241	4.81E-02
Ac-227	3.18E-02	Am-241	1.60E-03
Th-229	9.44E-05		

2.2 The Repository Sub-Model

The model compartments in this sub-model are shown in Figure 2.2.1. Radionuclides are leached from the waste into the concrete base and are then transported vertically in unsaturated flow to the unsaturated zone of the geosphere.

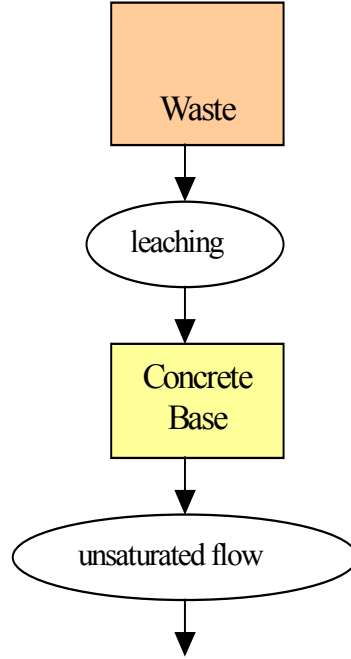


Figure 2.2.1 Compartments in the Repository Sub-Model.

The leaching rate from the waste in the repository depends on the flow rate through the waste and the physical and chemical properties of the waste and concrete base. Leaching occurs once the drums containing the waste fail.

For a given radionuclide, the net transfer (leaching) rate (y^{-1}), λ_{leach} , is:

$$\lambda_{leach} = \frac{q_{Adv}}{R D} = \frac{q_{In}}{\vartheta_w DR} \quad 2.2.1$$

where q_{Adv} is the advective velocity of water ($m y^{-1}$), q_{In} is the Darcy velocity of water through the medium ($m y^{-1}$) (equivalent to the infiltration rate), ϑ_w is the water filled porosity (-) of the medium, D is depth of the medium through which the radionuclide is transported (m), and R is the retardation coefficient (-) given by:

$$R = 1 + \frac{\rho Kd}{\vartheta_w} \quad 2.2.2$$

where ρ is the bulk density of the medium (kg m^{-3}) and Kd is the sorption coefficient of the medium ($\text{m}^3 \text{kg}^{-1}$).

q_{ln} and Kd are time dependent. A piece-wise constant performance of the cap covering the waste is assumed. It is also assumed that chemical degradation of the concrete base is linear, starting at closure (undegraded) and lasting until 1000 years after closure (totally degraded). Chemical degradation is represented by varying the Kd values linearly between the initial and degraded values.

Relevant model parameter values are given in Tables 2.2.1 and 2.2.2.

Table 2.2.1 Parameter Values for the Repository Sub-Model.

Parameter	Symbol	Units	Value
Compartments depths	D	m	9 (waste) 0.3 (concrete base)
Darcy Flux	q_{ln}	m y^{-1}	1.8E-3 $t < 100$ 1.8E-3 to 1.8E-2 linearly $100 < t < 500$ 1.8E-2 $t > 500$
Water-filled porosity	ϑ_w	-	0.2 (both waste and concrete base)
Bulk density	ρ	kg m^{-3}	1600 (both waste and concrete base)

Table 2.2.2 Sorption Coefficients for the Repository Sub-Model.

Element	Initial Value (m ³ kg ⁻¹)	Degraded Value (m ³ kg ⁻¹)	Element	Initial Value (m ³ kg ⁻¹)	Degraded Value (m ³ kg ⁻¹)
H	0E+0	0E+0	Ra	5E-2	5E-2
C	2E+0	2E-1	Ac	1E+0	2E-1
Ni	1E-1	1E-2	Th	5E+0	1E+0
Sr	1E-3	1E-3	Pa	5E+0	1E-1
Tc	1E-3	0E+0	U	2E+0	1E-1
I	1E-2	1E-3	Np	5E+0	1E-1
Cs	2E-2	2E-2	Pu	5E+0	1E+0
Pb	5E-1	5E-2	Am	1E+0	2E-1
Po	0E+0	0E+0			

2.3 The Unsaturated Geosphere Sub-Model

The model compartments in this sub-model are shown in Figure 2.3.1. The four strata in the unsaturated zone are here referred to simply as ‘Red Sand’, ‘Brown Sand’, ‘Clay’ and ‘Granite’. Radionuclides are transported in unsaturated groundwater flow from the Red Sand, to Brown Sand to Clay to Granite and then to the saturated zone of the geosphere. For simplicity the compartments that make up the different strata are not shown explicitly; in total there are 18 compartments in this sub-model.

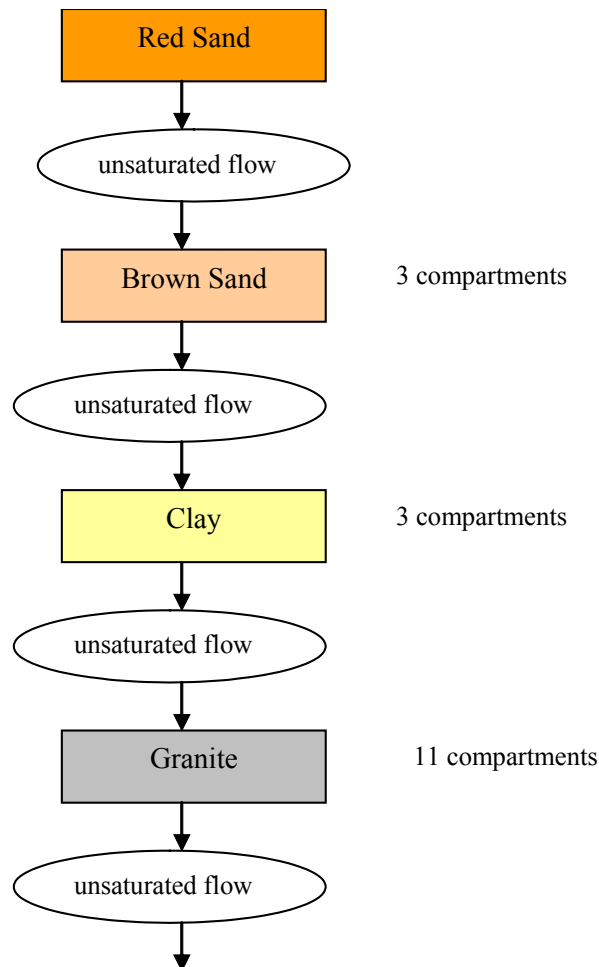


Figure 2.3.1 Compartments in the Unsaturated Geosphere Sub-Model.

Relevant model parameter values are given in Tables 2.3.1 and 2.3.2. The vertical Darcy flux through the unsaturated zone layers is the same as that for the Repository sub-model compartments, and the transfer rates follow equations (2.2.1) and (2.2.2).

Table 2.3.1 Parameter Values for the Unsaturated Zone Sub-Model.

Layer	Depth D (m)	Water-filled porosity v_w	Bulk density ρ (kg m ⁻³)
Red Sand	2.7	0.2	1989
Brown Sand	8.5	0.2	2230
Clay	8.0	0.2	2160
Granite	35.8	0.2	1683

Table 2.3.2 Sorption Coefficients for the Unsaturated Zone Sub-Model.

Element	Red Sand (m ³ kg ⁻¹)	Brown Sand (m ³ kg ⁻¹)	Clay (m ³ kg ⁻¹)	Granite (m ³ kg ⁻¹)
H	0E+0	0E+0	0E+0	0E+0
C	5.0E-3	5.0E-3	1.0E-3	5.0E-3
Ni	4.0E-1	4.0E-1	6.0E-1	4.0E-1
Sr	8.8E-3	7.1E-3	8.83E-3	5.5E-3
Tc	1.0E-4	1.0E-4	1.0E-3	1.0E-4
I	1.0E-3	1.0E-3	1.0E-3	1.0E-3
Cs	5.4E-1	3.4E-1	2.2E-1	2.6E-1
Pb	3.0E-1	3.0E-1	5.0E-1	3.0E-1
Po	1.5E-1	1.5E-1	3.0E0	1.5E-1
Ra	5.0E-1	5.0E-1	9.0E0	5.0E-1
Ac	3.4E-1	3.4E-1	7.6E0	3.4E-1
Th	3.0E0	3.0E0	6.0E0	3.0E0
Pa	3.4E-1	3.4E-1	7.6E0	3.4E-1
U	2.5E-3	6.8E-3	1.4E-3	3.0E-3
Np	3.4E-1	3.4E-1	7.6E0	3.4E-1
Pu	3.4E-1	3.4E-1	7.6E0	3.4E-1
Am	3.4E-1	3.4E-1	7.6E0	3.4E-1

2.4 The Saturated Geosphere Sub-Model

The model compartments in this sub-model are shown in Figure 2.4.1. There are nine Aquifer compartments together with a well compartment that is identical in structure to the other aquifer compartments. For simplicity only four of the total of ten compartments are shown in the Figure. Radionuclides are transported by saturated groundwater flow, and dispersion is represented as a diffusion-like process with the combination of 'forward' and 'backward' transfers between compartments giving the required radionuclide flux.

Water is taken from the well for irrigation and other purposes, represented by the two transfers shown in Figure 2.4.1.

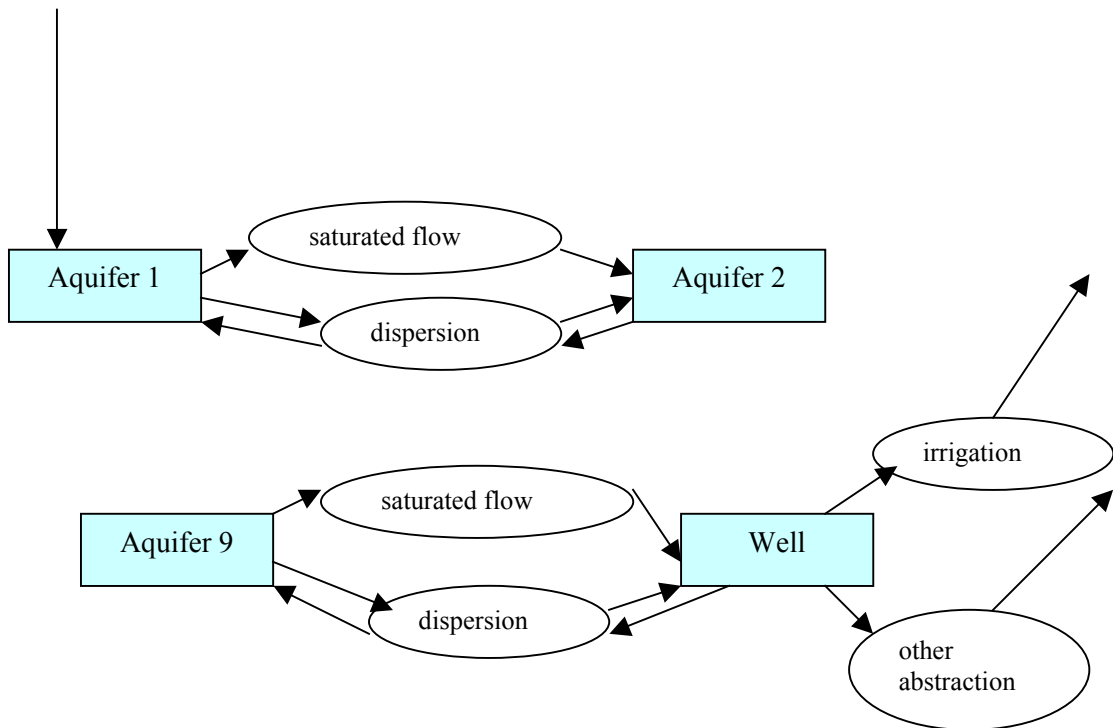


Figure 2.4.1 Compartments in the Saturated Geosphere Sub-Model.

In the saturated zone the Darcy velocity (q , in m y^{-1}) of the groundwater is calculated from the hydraulic conductivity of the medium (K , in m y^{-1}) and the hydraulic gradient through which water flows:

$$q = -K \frac{\partial H}{\partial x} \quad 2.4.1$$

where $\partial H/\partial x$ is the hydraulic gradient (-).

There are three transfers associated with each compartment:

$$\text{Advective flux from compartment i to compartment j} \quad \lambda_{A,ij} = \frac{q}{\vartheta_w L_i R} \quad 2.4.2$$

$$\text{Forward dispersion (i to j)} \quad \lambda_{D,ij} = \frac{a_x}{\Delta_x} \lambda_{A,ij} \quad 2.4.3$$

$$\text{Backward dispersion (j to i)} \quad \lambda_{D,ji} = \frac{a_x}{\Delta_x} \lambda_{A,ji} \quad 2.4.4$$

where $\lambda_{A,ij}$ is the rate of transfer of a contaminant by advection from compartment i to j (y^{-1}). $\lambda_{D,ij}$ is the rate of transfer of a contaminant by dispersion from compartment i to j (y^{-1}) with Δ_x is the distance over which the gradient in radionuclide concentration is calculated (m) and a_x the dispersion length.

The transfer rate of radionuclides from the Well compartment due to irrigation (y^{-1}), λ_{irrig} , is given by:

$$\lambda_{irrig} = \frac{A d_{irrig}}{\vartheta_w V_w R_w} \quad 2.4.5$$

where A is the area irrigated (m^2), d_{irrig} is the depth of effective irrigation water applied ($m y^{-1}$), ϑ_w is the water filled porosity (-) of the saturated zone from which the water is abstracted, V_w is the volume of the compartment representing the well (m^3), and R_w is the retardation coefficient (-) of the saturated zone (well).

The transfer rate of radionuclides due to abstraction of water for other purposes (y^{-1}), $\lambda_{non-irrig}$, is given by:

$$\lambda_{non-irrig} = \frac{V_{non-irrig}}{\vartheta_w V_w R_w} \quad 2.4.6$$

where $V_{non-irrig}$ is the volume of water abstracted for non-irrigation purposes plus loss due to interception and evaporation ($m^3 y^{-1}$).

Relevant model parameter values are given in Tables 2.4.1 and 2.4.2.

Table 2.4.1 Parameter Values for the Saturated Zone Sub-Model.

Parameter	Symbol	Units	Value
Lengths of each compartment	$L = \Delta x$	m	30
Volumes of each compartment	V	m ³	90
Hydraulic Conductivity	K	m y ⁻¹	1.8E3
Hydraulic gradient	$\partial H/\partial x$	-	0.1
Water-filled porosity	ϑ_w	-	0.25
Bulk density	ρ	kg m ⁻³	2000
Dispersion length	a_x	m	30
Area irrigated	A	m ²	1E5
Irrigation depth	d_{irrig}	m	0.05
Volume of water extracted for other purposes	$V_{non-irrig}$	m ³	3300

Table 2.4.2 Sorption Coefficients for the Saturated Zone Sub-Model.

Element	Kd (m ³ kg ⁻¹)	Element	Kd (m ³ kg ⁻¹)
H	0E+0	Ra	5.0E-1
C	5.0E-3	Ac	3.4E-1
Ni	4.0E-1	Th	3.0E+0
Sr	5.5E-3	Pa	3.4E-1
Tc	1.0E-4	U	3.0E-3
I	1.0E-3	Np	3.4E-1
Cs	2.6E-1	Pu	3.4E-1
Pb	3.0E-1	Am	3.4E-1
Po	1.5E-1		

3 AMBER and Ecolego Calculations

The original ISAM AMBER model was reviewed and an implementation error in the repository sub-model was found which was corrected. Revised AMBER calculations were undertaken for the intercomparison exercise with Ecolegoo.

3.1 Radionuclide Fluxes from the Repository

The first set of comparisons is for the flux of radionuclides from the repository sub-model into the unsaturated zone sub-model.

Radionuclide fluxes were calculated at fixed times: 150, 300, 1000 and 10 000 years. In addition, the time and magnitude of the peak flux was calculated for each radionuclide. Table 3.1.1 gives the details of these calculations. Fluxes calculated at specified times are quoted to four significant figures, whilst the time and magnitude of the peaks are quoted to just two significant figures because it is not straightforward to identify the exact location of the peak and the peak fluxes can therefore be expected to be less accurately calculated than fluxes at specified times.

The fluxes for the seven radionuclides that give the highest peak fluxes are shown in Figure 3.1.1. For these radionuclides, this figure is similar to Figure 6.2 in IAEA (2001), but is not exactly the same because more output times have been employed, and because of the error in the original ISAM calculations previously referred to.

It is not straightforward to provide an indication of the accuracy to be expected in the AMBER calculations. There is a global accuracy parameter of 1E-4 that is applied to the calculated compartment contents which can not be altered by the user. The calculated amount of a given radionuclide in any compartment will be accurate to at least 1E-4 times the maximum amount that has been calculated to be present in any compartment up to that time. This means that for radionuclides whose activities have been substantially reduced by radioactive decay, calculated amounts and fluxes can be expected to be less accurately calculated than radionuclides where radioactive decay has not significantly reduced activities.

Comparison of the AMBER and Ecolego calculations in Table 3.1.1 shows that agreement is generally excellent. In particular:

- The calculated peak fluxes and the times of the peaks agree to two significant figures.
- The calculated fluxes at specified times generally agree to at least three significant figures.

The exceptions to the second conclusion are:

- Agreement is sometimes less than three significant figures for radionuclides whose activities have been substantially reduced by radioactive decay. Examples are H-3 and Pu-241. These radionuclides have decayed by around 12 and 10 half-lives respectively by the time of the first comparison time (150 years).

- Fluxes at 1000 years where rapid change in the radionuclide fluxes can be seen due to the end of the concrete degradation period. Fluxes calculated by Ecolego are slightly less than those calculated by AMBER. It is not clear which of the two sets of calculations is the more accurate.

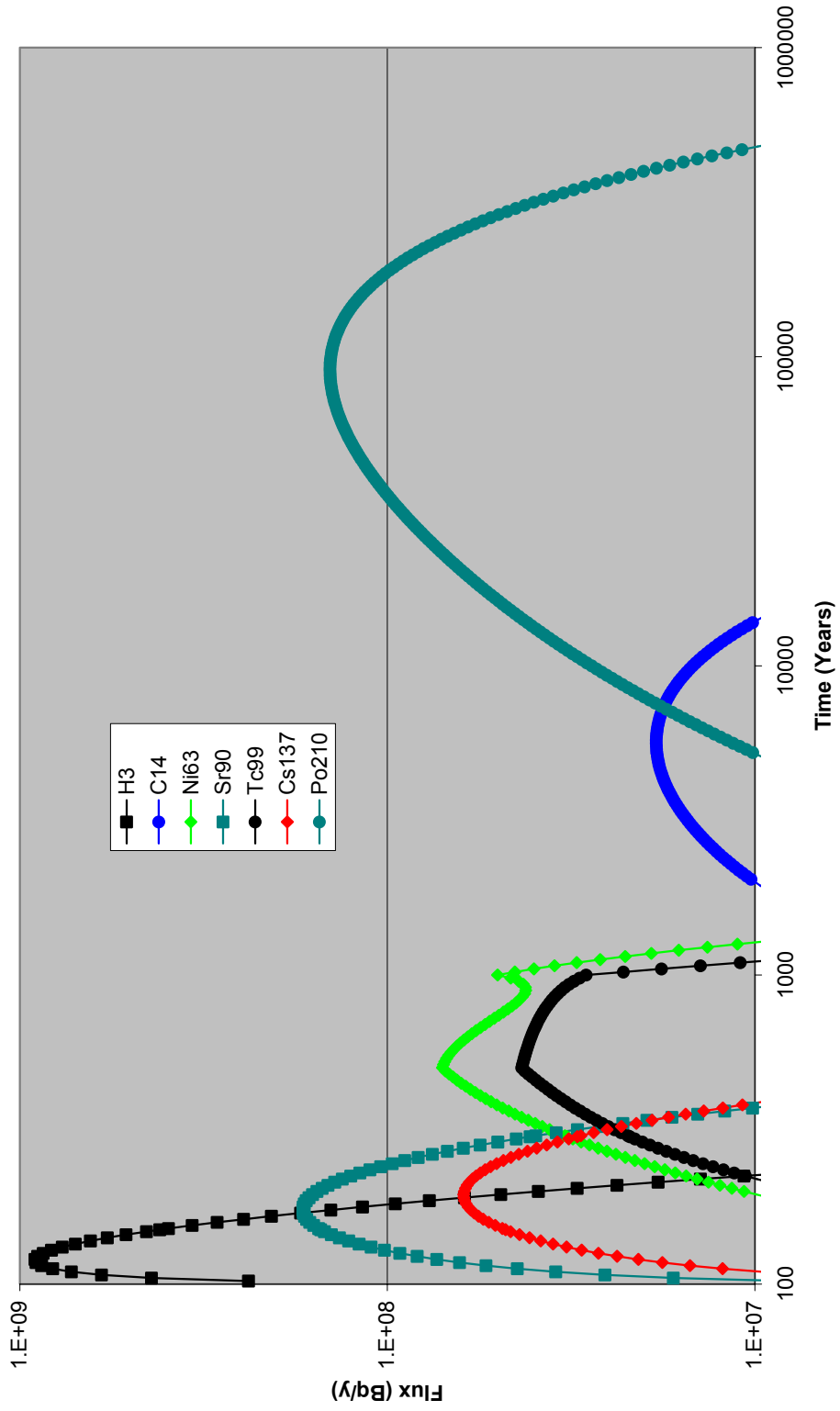


Figure 3.1.1 Fluxes from the Repository.

Table 3.1.1 Fluxes from the Repository (*AMBER calculations are in normal font; Ecolego calculations are in italic font*).

Radionuclide	Flux at 150 y (Bq y ⁻¹)	Flux at 300 y (Bq y ⁻¹)	Flux at 1000 y (Bq y ⁻¹)	Flux at 10 000 y (Bq y ⁻¹)	Peak (Bq y ⁻¹)	Peak Time (y)
H-3	4.161E8 <i>4.125E8</i>	1.551E5 <i>1.527E5</i>	- <i>3.257E-15</i>	-	9.1E8 <i>9.0E8</i>	120 <i>120</i>
C-14	2.496E2 <i>2.496E2</i>	6.942E2 <i>6.942E2</i>	2.257E6 <i>2.236E6</i>	1.477E7 <i>1.477E7</i>	1.9E7 <i>1.9E7</i>	5600 <i>5700</i>
Ni-59	2.022E2 <i>2.022E2</i>	5.640E3 <i>5.640E3</i>	1.357E6 <i>1.345E6</i>	7.461E5 <i>7.461E5</i>	2.2E6 <i>2.2E6</i>	1700 <i>1700</i>
Ni-63	3.428E6 <i>3.428E6</i>	3.242E6 <i>3.242E6</i>	5.013E7 <i>4.963E7</i>	- <i>1.188E-21</i>	7.1E7 <i>7.1E7</i>	500 <i>500</i>
Sr-90	1.517E8 <i>1.516E8</i>	4.08E7 <i>4.085E7</i>	2.391E0 <i>2.355E0</i>	-	1.7E8 <i>1.7E8</i>	170 <i>170</i>
Tc-99	2.070E6 <i>2.070E6</i>	2.189E7 <i>2.189E7</i>	2.878E7 <i>2.853E7</i>	-	4.3E7 <i>4.3E7</i>	500 <i>500</i>
I-129	5.832E3 <i>5.833E3</i>	1.438E5 <i>1.438E5</i>	5.294E6 <i>5.248E6</i>	2.404E2 <i>2.401E2</i>	5.3E6 <i>5.3E6</i>	1000 <i>1000</i>
Cs-137	4.771E7 <i>4.768E7</i>	3.043E7 <i>3.041E7</i>	3.325E1 <i>3.289E1</i>	-	6.2E7 <i>6.2E7</i>	190 <i>190</i>
U-234	1.292E0 <i>1.292E0</i>	3.729E1 <i>3.729E1</i>	3.204E4 <i>3.143E4</i>	5.551E5 <i>5.551E5</i>	5.6E5 <i>5.6E5</i>	10 000 <i>10 000</i>
U-238	1.291E0 <i>1.292E0</i>	3.729E1 <i>3.729E1</i>	3.204E4 <i>3.143E4</i>	5.551E5 <i>5.551E5</i>	5.6E5 <i>5.6E5</i>	10 000 <i>10 000</i>
Pu-238	2.410E-2 <i>2.410E-2</i>	2.012E-1 <i>2.012E-1</i>	1.163E-1 <i>1.158E-1</i>	-	3.7E-1 <i>3.7E-1</i>	500 <i>500</i>
Pu-239	1.177E-1 <i>1.177E-1</i>	3.200E0 <i>3.200E0</i>	4.572E2 <i>4.552E2</i>	8.253E3 <i>8.253E3</i>	1.1E4 <i>1.1E4</i>	22 000 <i>22 000</i>
Pu-241	1.739E-3 <i>1.730E-3</i>	3.494E-5 <i>3.468E-5</i>	- <i>1.114E-17</i>	-	1.8E-3 <i>1.8E-3</i>	140 <i>140</i>
Am-241	3.145E0 <i>3.145E0</i>	6.754E1 <i>6.754E1</i>	3.133E3 <i>3.119E3</i>	2.276E-2 <i>2.267E-2</i>	3.6E3 <i>3.6E3</i>	1300 <i>1300</i>
Th-230	3.259E-4 <i>3.259E-4</i>	2.021E-2 <i>2.021E-2</i>	1.133E1 <i>1.128E1</i>	3.824E3 <i>3.825E3</i>	1.9E4 <i>1.9E4</i>	8.9E4 <i>8.9E4</i>
Ra-226	4.879E-02 <i>4.880E-02</i>	3.197E+00 <i>3.197E+00</i>	4.189E+02 <i>4.189E+02</i>	6.838E+04 <i>6.838E+04</i>	3.6E5 <i>3.6E5</i>	9.1E4 <i>9.1E4</i>
Po-210	1.077E+02 <i>1.077E+02</i>	3.878E+03 <i>3.879E+03</i>	2.521E+05 <i>2.522E+05</i>	2.779E+07 <i>2.779E+07</i>	1.4E8 <i>1.4E8</i>	9.1E4 <i>9.1E4</i>
Pb-210	2.509E-03 <i>2.509E-03</i>	3.085E-01 <i>3.085E-01</i>	4.122E+02 <i>4.083E+02</i>	6.827E+04 <i>6.827E+04</i>	3.6E5 <i>3.6E5</i>	9.1E4 <i>9.1E4</i>

Radionuclide	Flux at 150 y (Bq y ⁻¹)	Flux at 300 y (Bq y ⁻¹)	Flux at 1000 y (Bq y ⁻¹)	Flux at 10 000 y (Bq y ⁻¹)	Peak (Bq y ⁻¹)	Peak Time (y)
U-235	1.042E-07 <i>1.042E-07</i>	5.594E-06 <i>5.595E-06</i>	1.596E-02 <i>1.566E-02</i>	2.468E+00 <i>2.468E+00</i>	6.8E0 <i>6.8E0</i>	5.1E4 <i>5.1E4</i>
Pa-231	3.921E-11 <i>3.922E-11</i>	4.957E-9 <i>4.957E-9</i>	1.299E-4 <i>1.243E-4</i>	2.783E-1 <i>2.784E-1</i>	3.7E0 <i>3.7E0</i>	8.5E4 <i>8.6E4</i>
Ac-227	2.725E-10 <i>2.725E-10</i>	2.703E-8 <i>2.703E-8</i>	5.917E-5 <i>5.899E-5</i>	1.386E-1 <i>1.386E-1</i>	1.8E0 <i>1.8E0</i>	8.5E4 <i>8.6E4</i>
Np-237	1.049E-05 <i>1.049E-05</i>	6.691E-04 <i>6.691E-04</i>	2.795E+00 <i>2.674E+00</i>	8.953E+01 <i>8.953E+01</i>	9.0E1 <i>9.0E1</i>	1.0E4 <i>1.0E4</i>
U-233	1.190E-08 <i>1.188E-08</i>	1.357E-06 <i>1.356E-06</i>	1.001E-02 <i>9.871E-03</i>	3.587E+00 <i>3.587E+00</i>	1.1E1 <i>1.1E1</i>	6.9E4 <i>6.9E4</i>
Th-229	1.376E-11 <i>1.374E-11</i>	3.459E-9 <i>3.455E-9</i>	1.848E-5 <i>1.840E-5</i>	1.147E-1 <i>1.147E-1</i>	1.1E0 <i>1.1E0</i>	8.1E4 <i>8.0E4</i>

3.2 Radionuclide Fluxes from the Unsaturated Zone

The second set of comparisons is for the flux of radionuclides from the unsaturated zone sub-model into the saturated zone sub-model.

Radionuclide fluxes were calculated at fixed times: 300, 1000 and 10 000 years (there is no significant flux for any radionuclide at 150 years). In addition, the time and magnitude of the peak flux was calculated for each radionuclide. Table 3.2.1 gives the details of these calculations. Fluxes are presented to the same number of significant figures as previously.

The fluxes for the four radionuclides that give the highest peak fluxes are shown in Figure 3.2.1. For these radionuclides, this figure is similar to Figure 6.4 in IAEA (2001), but is not exactly the same because of the previously noted differences.

Comparison of the AMBER and Ecolego calculations in Table 3.1.1 shows that agreement is generally excellent. In particular:

- The calculated peak fluxes and the times of the peaks agree to two significant figures.
- The calculated fluxes at specified times generally agree to around three significant figures, except for H-3 for the reasons discussed in Section 3.1.

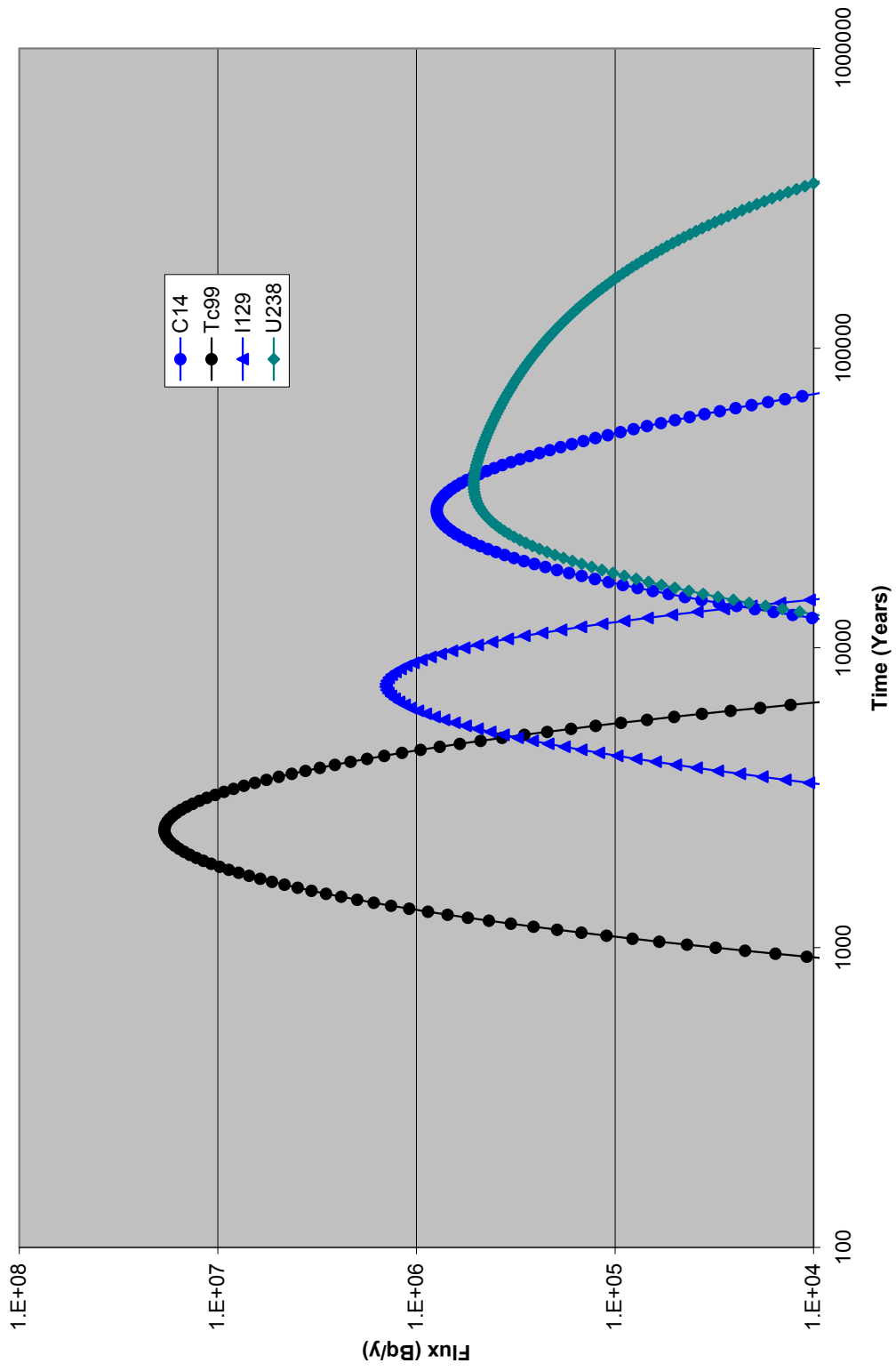


Figure 3.2.1 Fluxes from the Unsaturated Zone.

Table 3.2.1 Fluxes from the Unsaturated Zone (AMBER calculations are in normal font; Ecolego calculations are in italic font).

Radionuclide	Flux at 300 y (Bq y ⁻¹)	Flux at 1000 y (Bq y ⁻¹)	Flux at 10 000 y (Bq y ⁻¹)	Peak (Bq y ⁻¹)	Peak Time (y)
H-3	4.805E-7 <i>4.770E-7</i>	1.351E-12 <i>1.030E-12</i>	-	7.9E-4 <i>7.8E-4</i>	5.0E2 <i>5.0E2</i>
C-14	-	- <i>3.236E-17</i>	7.914E2 <i>7.924E2</i>	7.9E5 <i>7.9E5</i>	2.9E4 <i>2.9E4</i>
Ni-59	-	-	-	1.4E-2 <i>1.4E-2</i>	1.0E6 <i>1.0E6</i>
Ni-63	-	-	-	-	-
Sr-90	-	-	-	-	-
Tc-99	8.785E-13 <i>8.896E-13</i>	3.115E+04 <i>3.118E+04</i>	1.691E+00 <i>1.635E+00</i>	1.9E7 <i>1.9E7</i>	2.5E3 <i>2.5E3</i>
I-129	-	1.792E-06 <i>1.805E-06</i>	5.740E+05 <i>5.742E+05</i>	1.4E6 <i>1.4E6</i>	7.4E3 <i>7.5E3</i>
Cs-137	-	-	-	-	-
U-234	-	- <i>1.254E-17</i>	6.918E+02 <i>6.924E+02</i>	5.1E5 <i>5.1E5</i>	3.5E4 <i>3.5E4</i>
U-238	-	- <i>1.253E-17</i>	6.917E+02 <i>6.923E+02</i>	5.1E5 <i>5.1E5</i>	3.5E4 <i>3.5E4</i>
Pu-238	-	-	-	-	-
Pu-239	-	-	-	4.7E-12 <i>4.7E-12</i>	5.1E5 5.2E5
Pu-241	-	-	-	-	-
Am-241	-	-	-	-	-
Th-230	-	-	4.835E-03 <i>4.843E-03</i>	2.0E2 <i>2.0E2</i>	1.2E5 <i>1.2E5</i>
Ra-226	-	-	6.678E-03 <i>6.694E-03</i>	1.2E3 <i>1.2E3</i>	1.2E5 <i>1.2E5</i>
Po-210	-	-	2.124E-02 <i>2.129E-02</i>	4.0E3 <i>4.0E3</i>	1.2E5 <i>1.2E5</i>
Pb-210	-	-	1.063E-02 <i>1.066E-02</i>	2.0E3 <i>2.0E3</i>	1.2E5 <i>1.2E5</i>
U-235	-	-	6.735E-04 <i>6.743E-04</i>	7.0E0 <i>7.0E0</i>	7.2E4 <i>7.2E4</i>
Pa-231	-	-	9.232E-08 <i>9.251E-08</i>	4.8E-2 <i>4.8E-2</i>	1.2E5 <i>1.2E5</i>
Ac-227	-	-	8.906E-08 <i>8.925E-08</i>	4.8E-2 <i>4.8E-2</i>	1.2E5 <i>1.2E5</i>

Radionuclide	Flux at 300 y (Bq y ⁻¹)	Flux at 1000 y (Bq y ⁻¹)	Flux at 10 000 y (Bq y ⁻¹)	Peak (Bq y ⁻¹)	Peak Time (y)
Np-237	-	-	-	1.2E-4 <i>1.2E-4</i>	1.0E6 <i>1.0E6</i>
U-233			1.052E-03 <i>1.054E-03</i>	3.3E1 <i>3.3E1</i>	1.7E5 <i>1.7E5</i>
Th-229			6.665E-08 <i>6.680E-08</i>	3.5E-2 <i>3.5E-2</i>	1.9E5 <i>1.9E5</i>

3.3 Well Water Concentrations

The third set of comparisons is for the concentration of radionuclides in well water in the saturated zone sub-model.

Radionuclide concentrations were calculated at fixed times: 1000 and 10 000 years (there are no concentrations for any radionuclide at 150 or 300 years). In addition, the time and magnitude of the peak concentration were calculated for each radionuclide. Table 3.3.1 gives the details of these calculations. Concentrations are presented to the same number of significant figures as previously.

The concentrations for the four radionuclides that give the highest peak fluxes are shown in Figure 3.3.1; these are the same radionuclides that gave the highest peak fluxes from the unsaturated zone in Section 3.2. For these radionuclides, this figure is similar to Figure 6.6 in IAEA (2001), but is not exactly the same because of the previously noted differences.

Comparison of the AMBER and Ecolego calculations in Table 3.3.1 shows that agreement is generally excellent. In particular:

- The calculated peak fluxes and the times of the peaks agree to two significant figures.
- The calculated fluxes at specified times generally agree to around three significant figures.

This degree of agreement between the two sets of calculations is impressive given the large number of compartments in the model and the inclusion of decay chains with up to six members.

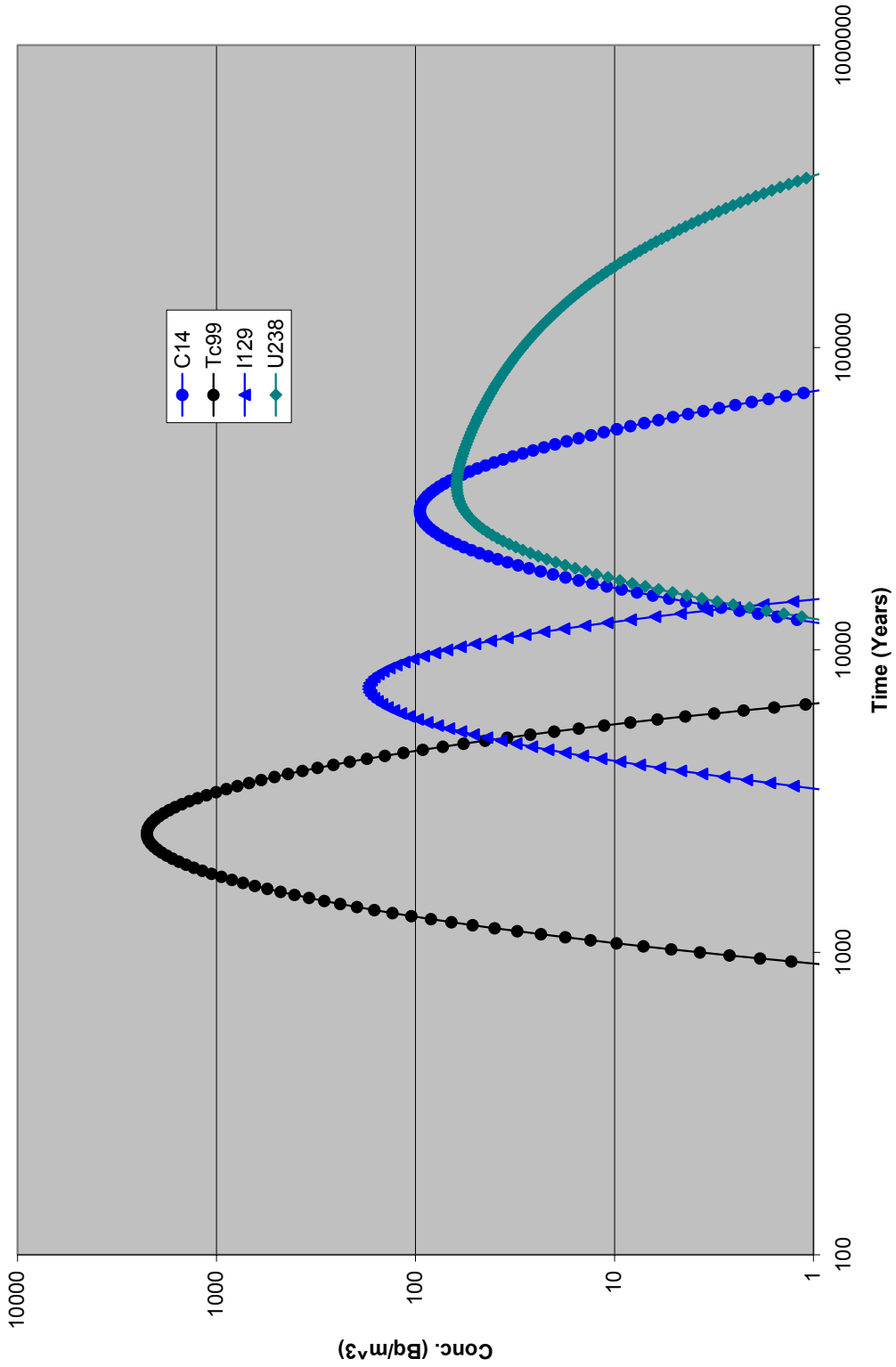


Figure 3.3.1 Well Water Concentrations.

Table 3.3.1 Well Water Concentrations (*AMBER calculations are in normal font; Ecolego calculations are in italic font*).

Radionuclide	Conc. at 1000 y (Bq m ⁻³)	Conc. at 10 000 y (Bq m ⁻³)	Peak (Bq m ⁻³)	Peak Time (y)
H-3	- <i>2.616E-11</i>	- <i>1.230E-12</i>	- <i>9.3E-8</i>	- <i>5.0E2</i>
C-14	-	9.360E-02 <i>9.372E-02</i>	9.5E1 <i>9.5E1</i>	2.9E4 <i>2.9E4</i>
Ni-59	-	-	1.7E-6 <i>1.7E-6</i>	1.0E6 <i>1.0E6</i>
Ni-63	-	-	-	-
Sr-90	-	-	-	-
Tc-99	3.719E+00 <i>3.723E+00</i>	2.040E-04 <i>1.973E-04</i>	2.2E3 <i>2.2E3</i>	2.5E3 <i>2.5E3</i>
I-129	2.008E-10 <i>2.023E-10</i>	6.929E+01 <i>6.932E+01</i>	1.7E2 <i>1.7E2</i>	7.4E3 <i>7.5E3</i>
Cs-137	-	-	-	-
U-234	-	8.253E-02 <i>8.260E-02</i>	6.2E1 <i>6.2E1</i>	3.5E4 <i>3.5E4</i>
U-238	-	8.251E-02 <i>8.259E-02</i>	6.2E1 <i>6.2E1</i>	3.5E4 <i>3.5E4</i>
Pu-238	-	-	-	-
Pu-239	-	-	- <i>5.5E-16</i>	- <i>5.2E5</i>
Pu-241	-	-	-	-
Am-241	-	-	-	-
Th-230	-	5.771E-07 <i>5.781E-07</i>	2.4E-2 <i>2.4E-2</i>	1.2E5 <i>1.2E5</i>
Ra-226	-	7.961E-07 <i>7.979E-07</i>	1.4E-1 <i>1.4E-1</i>	1.2E5 <i>1.2E5</i>
Po-210	-	2.532E-06 <i>2.538E-06</i>	4.8E-1 <i>4.8E-1</i>	1.2E5 <i>1.2E5</i>
Pb-210	-	1.267E-06 <i>1.270E-06</i>	2.4E-1 <i>2.4E-1</i>	1.2E5 <i>1.2E5</i>
U-235	-	8.029E-08 <i>8.039E-08</i>	8.4E-4 <i>8.4E-4</i>	7.2E4 <i>7.2E4</i>
Pa-231	-	1.101E-11 <i>1.103E-11</i>	5.8E-6 <i>5.8E-6</i>	1.2E5 <i>1.2E5</i>

Radionuclide	Conc. at 1000 y (Bq m ⁻³)	Conc. at 10 000 y (Bq m ⁻³)	Peak (Bq m ⁻³)	Peak Time (y)
Ac-227	-	1.062E-11 <i>1.064E-11</i>	5.8E-6 <i>5.8E-6</i>	1.2E5 <i>1.2E5</i>
Np-237	-	-	1.5E-8 <i>1.5E-8</i>	1.0E6 <i>1.0E6</i>
U-233	-	1.253E-07 <i>1.255E-07</i>	4.0E-3 <i>4.0E-3</i>	1.7E5 <i>1.7E5</i>
Th-229	-	7.947E-12 <i>7.965E-12</i>	4.2E-6 <i>4.2E-6</i>	1.9E5 <i>1.9E5</i>

4 Conclusions

The comparisons between the AMBER and Ecolego calculations for the ISAM vault safety case have shown excellent agreement. Calculations at specified times generally agree to around three significant figures, and calculations of peak radionuclide fluxes and concentrations agree to two significant figures. This agreement is particularly good given the large number of model compartments and the inclusion of decay changes of up to six members.

The most important situation where agreement may not be as good as that generally found is where radionuclides have been subject to substantial losses due to radioactive decay; at times after the production of the radionuclide that are very much greater than the radionuclide half-life.

References

Avilia, R, Broed R. and Pereira, A (2003). Ecolego - a Toolbox for Radioecological Risk Assessments. International Conference on the Protection of the Environment from the Effects of Ionising Radiation, 6 –10 October 2003, Stockholm, Sweden.

Enviros and Quintessa Ltd (2003). AMBER version 4.5.

IAEA (2001). ISAM, The International Programme for Improving Long Term Safety Assessment Methodologies for Near Surface Radioactive Waste Disposal Facilities: Vault Safety Case Report. ISAM Document version 1.3, August 2001: working material.

SKB (1999). Deep Repository for Spent Fuel. SR97- Post-closure safety, volumes I and II. SKB report TR-99-06.

SKI and SSI (2003). AMBER and Ecolego Intercomparisons using Calculations from SR97.

www.ski.se
www.ssi.se

STATENS KÄRNKRAFTINSPEKTION
Swedish Nuclear Power Inspectorate

POST/POSTAL ADDRESS SE-106 58 Stockholm
BESÖK/OFFICE Klarabergsviadukten 90
TELEFON/TELEPHONE +46 (0)8 698 84 00
TELEFAX +46 (0)8 661 90 86
E-POST/E-MAIL ski@ski.se
WEBBPLATS/WEB SITE www.ski.se

STATENS STRÅLSKYDDSINSTITUT
Swedish Radiation Protection Authority

POST/POSTAL ADDRESS SE-171 16 Stockholm
BESÖK/OFFICE Solna strandväg 96
TELEFON/TELEPHONE +46 (0)8 729 71 00
TELEFAX +46 (0)8 729 71 08
E-POST/E-MAIL ssi@ssi.se
WEBBPLATS/WEB SITE www.ssi.se